

PERFORMANCE ANALYSIS OF HYBRID ELECTRIC VEHICLE WITH ELECTRIC DOUBLE LAYER CAPACITOR UNDER SHORT CIRCUIT FAULT

IBRAHIM SEFIK¹ AND DIMAS ANTON ASFANI²

¹Automotive Technology Department
Tubitak MRC Energy Institute
Baris Mah. Dr. Zeki Acar Cad. No:1 P.K. 21 41470 Gebze, Kocaeli, Turkey
ibrahim.sefik@tubitak.gov.tr

²Jurusan Teknik Elektro
Institut Teknologi Sepuluh Nopember
Jurusan Teknik Elektro, Kampus ITS Keputih Sukolilo, Surabaya 60111, Indonesia
anton@ee.its.ac.id

Received February 2014; revised June 2014

ABSTRACT. *Energy management system (EMS) studies are one of the most popular issues in (Hybrid Electric Vehicle) HEV technology and research. However, the fault and failure analysis of HEV is also important regarding to safety and reliability. Because there occurs various types of faults in several vital parts of HEV drive-trains which can have impact on providing a healthy operation and consequently result in a low performance or malfunction in whole system. There are many studies related to vehicle technology regarding the diagnosis and fault detection in HEVs. Nevertheless, only a few of them concern short circuit fault. In this paper, model analysis of HEV under the short circuit fault symptoms is presented to get insight of the fault effect on the HEV performance. Accordingly, high impedance short circuit fault is simulated occurring at DC electric system. Moreover, Electric Double Layer Capacitor (EDLC)-battery power source is proposed in order to suppress short circuit fault effect in the system and to increase the HEV performance since EDLC behaves like a rapid charging/discharging buffer. We utilize a parallel-series type HEV simulation model which is developed in Matlab/Simulink environment including a short circuit fault case. Developed model of EDLC-battery pack hybrid power source is tested in this HEV simulation model and the impact of EDLC on short circuit fault and the whole system performance is analyzed.*

Keywords: Hybrid electric vehicle (HEV) modeling, Energy management system (EMS), Parallel-series type power-train, Electric double layer capacitor (EDLC), Short circuit fault, Hybrid power source

1. Introduction. According to International Energy Agency (IEA)'s latest report of CO₂ Emission From Fuel Combustion all over the globe, 23% of total CO₂ emission stems from the transportation including motor vehicles as shown in Figure 1 [1]. Therefore, in recent years since CO₂ emission is directly related to global warming and economical use of energy problems, Hybrid Electric Vehicles (HEV) which has less CO₂ emission and higher energy efficiency in comparison with conventional vehicles are developed as a countermeasure [2].

Inside of the HEVs, depending on the vehicles running condition, power management is achieved among the parts such as engine, motor, battery, and generator. As a method in order to maintain running efficiency and to increase fuel efficiency for HEVs, mainly there are 3 types of drive-trains patterns such as series, parallel and parallel-series [3]. When looking into detail of any drive-train type, a certain combination of internal combustion (IC) engine, motor, battery and generator is found. Among those types, parallel-series

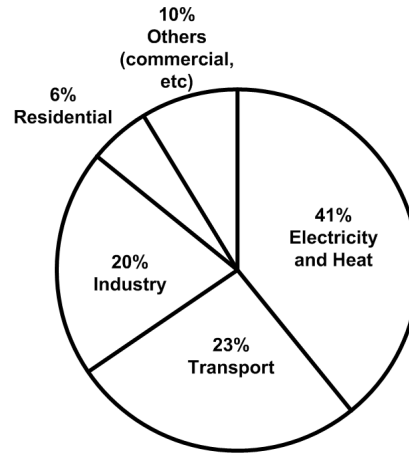


FIGURE 1. Estimated CO₂ emissions in the world

hybrid drive-train of a HEV simulation which is developed with Matlab/Simulink tool is considered as an experimental environment in this study.

A HEV contains a battery pack consisting of non-spillable 30 low voltage Nickel-Metal-Hydride (NiMH) battery modules that power the high voltage electrical subsystem with direct current (DC) [4]. In the development and usage process of a HEV, according to hybrid electric vehicle report of investigation, several faults including short circuit give severe damage to vehicle and endanger the passengers [5]. Some of short circuit faults occur in the battery pack caused by built-up heat together with voltage surge or loose connection between battery cells that led to insulation failure [6]. This fault occurs even the HEV battery pack is structured with a high voltage fuse providing the short circuit protection [4].

The study model of HEV contains two inverters and a DC/DC converter modules which are composed of several Isolated Gate Bipolar Transistors (IGBT) and Free Wheeling Diodes (FWD). In this model, water cooling is applied on the power modules so that their maximum junction temperature swing is around 50°C. Temperature rise may cause severe results [7]. Moreover, hard environment conditions can add up plus risks. Furthermore, one another important issue about IGBT containing models is high surge voltage during the IGBT switching at high voltages stemming from the sharp changes in current and stray inductance. In the study system, IGBT containing inverter modules increase the voltage to feed motor. Accordingly, high voltages may decrease the robustness of the system against short circuit which is indispensable. However, generally the cause to the short circuit fault is partial deformation of battery pack separators, which creates local hot spots causing insulation failure. Especially in case of polyethylene or polypropylene separators, this local hot spots give major damages to the separator since they undergo a shrinkage increasing the short circuit area. Besides, separator deformation can also be caused by an external mechanical intervention such as in a crush. Short circuit fault is also possible to be encountered due to internal breakdown of battery cell because of an impurity or incorrect power management topology [8].

Another interesting research topic in EV/HEV is utilization of ultra-capacitor or ELDC to increase the electric power source performances. When comparing a battery with an ultra-capacitor such as EDLC, batteries have drawbacks of low power density and limited charge/discharge cycle life-times as well as long charging times and high temperature dependence. For the compensation of battery pack disadvantages, EDLCs with high power densities and higher repetitive charge/discharge life-times are required [9]. Accordingly,

EDLCs which are utilized in charge sustaining hybrid vehicles such as HEVs have low energy density ranging from 5 to 10 Wh/kg while having high power densities changing between 1-2 kW/kg [10]. Introductions of ultra capacitor studies to EV/HEV applications date back to about 1990 and for the reasons counted above, these studies are mostly concentrated on providing better power and life-cycle characteristics. Therefore, for most HEV applications, EDLC power capability is measured by high efficient power density [10]. Thus, with an EDLC in the system, stable DC bus voltage can be easily obtained and power fluctuations during the short circuit faults can considerably be cleared off and whole system power quality is remarkably improved. Also, since the battery pack on a HEV is an electrochemical system which goes through an early deterioration by high charge/recharge cycle times, by compensating the harmonic components of fluctuating power by means of the proposed EDLC system, smooth component of power is supplied. Consequently, decrease in high charge/recharge cycle times [11] yields a longer life-time for the battery pack [9]. In order to know some improvement and performance effect, several simulation models of HEV are already in use by researchers [12-20]. Some of them are considering the utilization of ultra capacitor to increase the performance [16-19]. The effect of short circuit fault in the electric system is also investigated [15,20]. However, the comprehensive analysis including the effect of EDLC during normal acceleration, deceleration and short circuit fault is not yet investigated so this paper focuses on this analysis including the effect of capacitor size.

In this study, HEV model considering ELDC is proposed. Using this model, the HEV electrical system performance is evaluated including the DC voltage stability and battery. Several operation cases of HEV during normal and faulty conditions are simulated. Normal operation cases are consisting of acceleration and deceleration of the vehicle. While the faulty operation is modeled as short circuit faults in DC bus to represent the HEV accident event in June 2008 at Arizona, US [5]. During simulation cases, several variables are evaluated consisting of fluctuations in battery DC bus voltage and power, battery state of charge (SOC), engine power and motor power. The result shows that the ELDC gives the excellent performance by reducing DC voltage fluctuation during normal acceleration, deceleration and fault. Moreover, battery SOC can be improved that yields a longer life-time of battery.

2. Parallel-Series Type Hybrid Drive-Train. A series-parallel hybrid drive-train structure is composed of both series and parallel drive-trains as shown in Figure 2. This type of drive-train is the most common and commercially adopted topology among car manufacturers and also well-known with incorporating a power split mechanism called planetary gear system that transfers power from the engine to the wheels either electrically and mechanically [12]. As for the series-parallel hybrid drive-train operation, depending on the driving requirements and battery SOC, operating conditions are split into six phases. In the engine start phase, only the battery provides traction power to the vehicle and the IC engine is the off mode. In the acceleration phase, the IC engine and battery fed electric motor together supply the traction power. Besides, generator supplies power and both motor and generator are controlled to maintain the gear ratio by using planetary gear system. In the cruising phase, only the IC engine supplies the required traction power to the wheels and the electric motor is in the off mode. During braking, electric motor behaves like a generator and kinetic energy loss is stored back to the battery back. During driving, if the battery needs to be charged, IC engine drives also the generator to recharge the battery. When the vehicle stops, the battery can be still charged by the IC engine via the generator. This multi-phase operational feature is given to the vehicle by its planetary gear system.

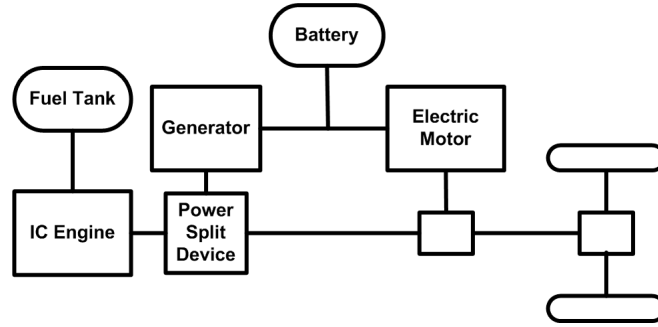


FIGURE 2. Series-parallel drivetrain

3. **HEV Simulation Model with ELDC.** In this section, utilized HEV power-train model composed of 5 main parts is presented as shown in Figure 3. HEV Modelling is structured by using physical modelling support tools such as Simulink, SimDriveline and SimPowerSystems. In this model, energy management system represents the control algorithm which is described in control subsystem components and optimizes hybrid system's energy efficiency. Electric subsystem utilizes the permanent magnet type electric motor, generator, inverter, bidirectional DC/DC converter and battery. Internal combustion (IC) engine gives the rotation rate of gasoline engine and its characteristics which determines the output torque through throttle position. Power split mechanism is a planetary gear system which splits engine output power and delivers it electrically and mechanically. Finally, vehicle subsystem represents vehicle's two-way characteristics, front and rear tires' friction characteristics and speed reduction gear, etc.

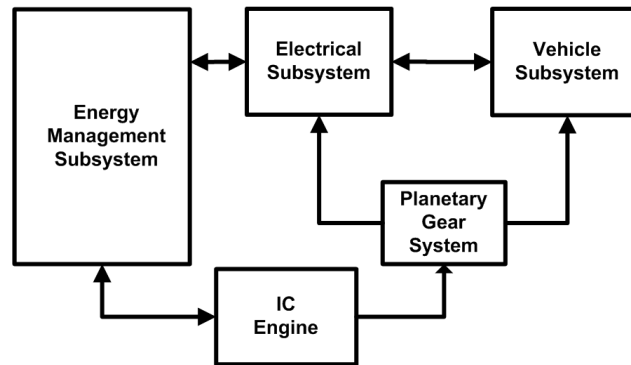


FIGURE 3. HEV simulation model

3.1. **Energy management subsystem.** This system provides optimum management algorithm among IC engine, electric motor and generator by creating reference signals. These signals are calculated based on the driver's acceleration pedal signal whose value is changing from +100% to -100% and the vehicle speed. Here, while positive numbers correspond to acceleration, negative numbers correspond to braking. Energy management system is mainly composed of three subsystems which are system operation part, motor reference signals calculation part and generator reference signals calculation part as can be seen in Figure 4.

In system operation part, activation/deactivation and power management for generator, engine, motor and battery are realized. Here, the most efficient driving condition is estimated based on acceleration pedal position, vehicle speed and required power for the HEV propulsion. Then enabling signals are created for engine, motor and generator

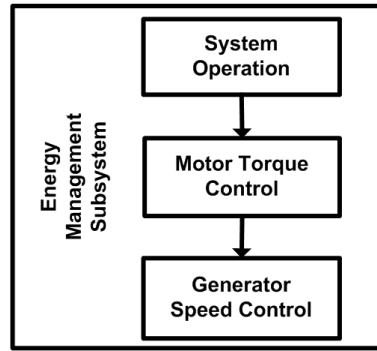


FIGURE 4. Energy management system

drives. Also, battery power calculation is carried out based on battery SOC, voltage and current values. In motor reference signals calculation part, motor's reference torque signal together with the engine throttle position reference signal are generated. Also, engine output calculation is done. HEV reference torque, engine output torque, generator and motor angular speed and battery output power which is created in system operation part are taken into account when generating motor reference torque signal. Engine reference throttle position and output power is obtained from HEV. In generator reference signals calculation part, optimum speed reference signal for generator is created based on engine reference angular speed which is coming from the second part and motor angular speed.

3.2. Mechanical system. Mechanical subsystem of utilized HEV simulation model is mainly composed of internal combustion engine, power split device representing a planetary gear system which splits power coming from IC engine and vehicle subsystem in which vehicle body is modelled. Modelling work of internal combustion engine is a quite different study area requiring a deep knowledge of mechanical engineering so it is skipped and interested readers are advised to read [21] for further knowledge. Power split device and vehicle body are created by using ready-to-use SimDriveline blocks as well as Simulink offered blocks together in mechanical subsystem and physical dynamics of these components are given in detail in following Sections 3.2.1 and 3.2.2.

3.2.1. Power split device. Series-parallel hybrid drive-train structure of this study model is composed of both series and parallel drive-trains and shows the features of both types. This type of drive-train incorporates power-split devices called Planetary Gear Unit (PGU) transferring the power from engine to the wheels either electrically and mechanically. So this means that there exists also an additional direct mechanical transmission link in series-parallel drive train configuration more complex and expensive when comparing with the others. Nevertheless, recent hybrid vehicle technologies adopt this type. As can be seen in Figure 5, power split device is composed of three gears such as Carrier, Ring and Sun. Carrier is connected to the IC engine and it plays a role of input to this PGU unit. Ring is connected to mechanical line in order to combine with motor and supply driving torque to the wheels together. Sun is connected to the generator and help the vehicle generate power to charge battery pack in need. When the generator is off, PGU turns out to be a simple transmission box with a fixed gear ratio. Torque relation of motor, generator and IC engine is calculated through Equation (1) in the model. R , C and S indicate radius of each gear. Dynamics details and further information related to PGU can be found in [22].

$$2C\omega_C = S\omega_C + R\omega_R \quad (1)$$

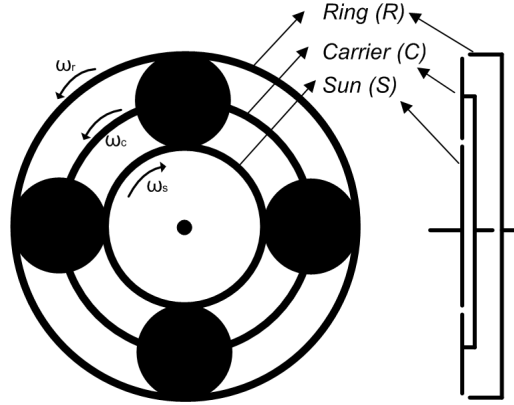


FIGURE 5. Power split device

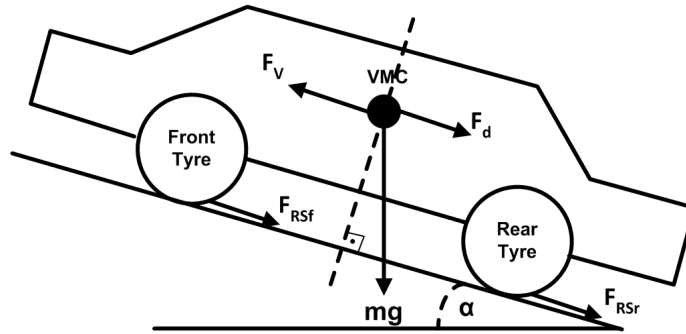


FIGURE 6. Vehicle model

3.2.2. *Vehicle subsystem.* Vehicle subsystem of this study model is shown in Figure 6. This subsystem models longitudinal vehicle dynamics based on the two-axle and four wheels which are moving forward and backward along the horizontal axis. VMC is vehicle mass center. Calculation of Equation (2) derived from Newton's second law is performed while taking VMC point as reference.

$$m \frac{dv}{dt} = F_V + F_d + F_{RS} - mg \sin(\alpha) \quad (2)$$

$$F_d = -\frac{1}{2} C_d \rho A V^2 \text{sgn}(v) \quad (3)$$

$$F_{RS} = F_{RSf} + F_{RSr} = mg \cos(\alpha) C_g \quad (4)$$

3.3. **Electric subsystem.** Electrical subsystem of utilized HEV simulation model is shown in Figure 7. This subsystem is mainly composed of battery, bidirectional DC/DC converter, inverters, motor and generator. Some of these components are offered by SimPower-Systems (Electrical Systems Modelling Support Tool) as ready-to-use blocks. Four different control units are also structured in this subsystem for charge/recharge control of battery, step-up control for bidirectional DC/DC converter, motor torque control and generator speed control. Permanent magnet type synchronous machines are used for motor (500 V, 50 kW, 6000 rpm, 8-pole) and generator (500 V, 30 kW, 13000 rpm, 2-pole) then they are interfaced by three-phase inverter. On the other side of bidirectional DC/DC converter which is a two-quadrant chopper circuit, there exists battery unit. Bidirectional DC/DC converter regulates 200 V at the battery side to the DC bus that feeds the AC motor at 500 V. It also gives HEV the feature of operating in all-electric,

TABLE 1. Symbols

Symbol	Meaning	Unit	Value
m	Vehicle Mass	kg	1360
v	Vehicle Speed	km/h	0 to 80
F_V	Vehicle Force	N	Equation (2)
F_d	Aerodynamic Drag Force	N	Equation (3)
F_{RS}	Rolling Resistance	N	Equation (4)
α	Road Inclination Angle	%	10%
C_d	Aerodynamic Drag Coefficient	$N \cdot s^2 / kg \cdot m$	0.26
C_g	Ground Friction Coefficient	$N \cdot s^2 / kg \cdot m$	0.7
ρ	Air Mass Density	kg / m^3	1.2
A	Vehicle Frontal Area	m^2	2.57
g	Gravitational Acceleration	m / s^2	9.81

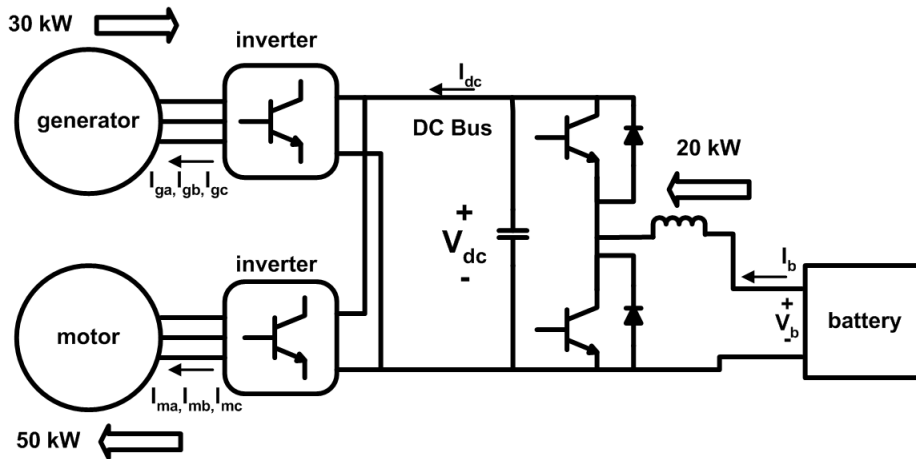


FIGURE 7. Electric subsystem

electric-assist and fuel-powered modes depending on the battery SOC. Besides, regenerative braking power recharges the battery during deceleration of HEV through bidirectional DC/DC converter. Battery pack in the system is represented by the most popular types of rechargeable batteries. Generic dynamic model parameterization is implemented in modelling of this battery. Average value modelling is used for motor and generator models as well as bidirectional DC/DC converter block in order to shorten the simulation run time since this option allows longer simulation time steps. Since details of permanent magnet machines modellings are beyond the scope of this study, their modelling details are skipped and readers are advised to refer to textbook [23].

3.3.1. DC/DC converter operation and modelling. DC/DC converter of this study model can work bidirectionally since battery charge and discharge are required depending on the HEV driving conditions. Therefore, two-quadrant bidirectional converter is operated in buck and boost modes as can be seen in Figure 8 and Figure 9 respectively.

When battery charging is needed, converter behaves like a buck converter, keeps IGBT2 and FWD1 in off mode and draws power from DC bus. Reversely, when discharge of battery is needed, converter switches to boost converter mode, turns IGBT1 and FWD2 off and releases power to DC bus in order to feed motor. When modelling this bidirectional DC/DC converter, average switch modelling which is a type of average value modelling

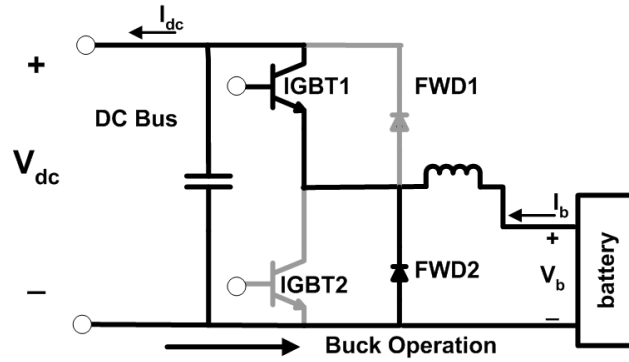


FIGURE 8. Buck operation of DC/DC converter circuit diagram

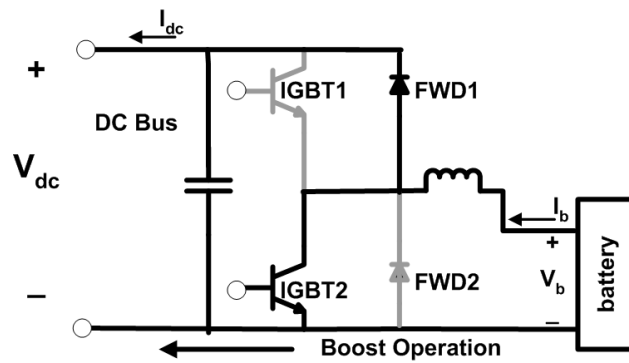


FIGURE 9. Boost operation of DC/DC converter circuit diagram

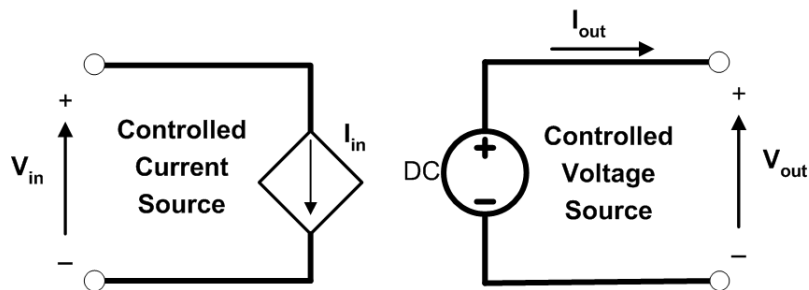


FIGURE 10. DC/DC converter switching elements average switch model

method is applied. In this modelling method, switching components such as diodes and IGBTs in the system are represented by controlled current and voltage sources [24,25].

Two-quadrant DC/DC converter average switch model is shown in Figure 10. Depending on the buck and boost operations, DC source side and load side are represented by controlled current and controlled voltage source respectively. Here, α is IGBT switching duty cycle which is created at DC/DC converter's voltage controller in order to obtain desired output voltage. Accordingly, Equations (5) and (6) give output voltage and output current respectively.

$$V_{out} = \alpha V_{in} \tag{5}$$

$$I_{in} = \alpha I_{out} \tag{6}$$

Voltage controller, as shown in Figure 6, is the control system for obtaining desired output voltage from DC/DC converter. Regarding IGBT switching elements in DC/DC

converter, it is necessary to generate gate signals to control their on-off timings. *CYCLE1* and *CYCLE2* are duty cycles which are calculated due to Equations (7) and (8).

$$CYCLE1 = 0.5(E_c + 1) = \alpha \tag{7}$$

$$\begin{aligned} CYCLE2 &= 1 - 0.5(E_c + 1) \\ &= 1 - CYCLE1 = 1 - \alpha \end{aligned} \tag{8}$$

3.3.2. *Three-phase inverter operation and modelling.* Three-phase inverter, shown in Figure 12, is used in this study model. Inverter is connecting motor and generator to DC bus as can be seen in Figure 7. For the operation of three-phase inverter, well-known pulse width modulation (PWM) technique is applied. This technique is commonly used to control and obtain suitable power and voltages at electrical machines input terminals. Basically in this technique, duty cycles which are describing proportion of on-off timings for switching elements in three-phase inverter are calculated based on the width of pulses generated by the comparison of a high-frequency triangular signal and fundamental frequency sinusoidal reference signal. When modelling this three-phase inverter circuit, average switch modelling technique is utilized as well [26]. For the explanation of modelling phenomenon, three-phase inverter which interfaces motor with DC bus in Figure 7 is selected since it is very similar also in case of generator interfaced inverter.

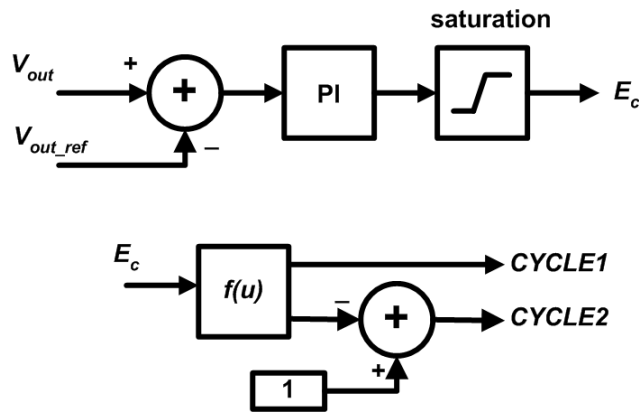


FIGURE 11. DC/DC converter voltage controller

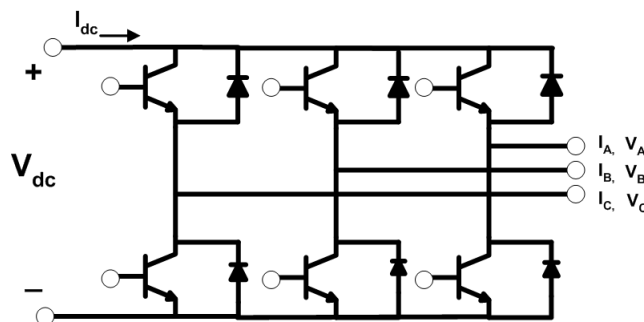


FIGURE 12. Three-phase inverter circuit diagram

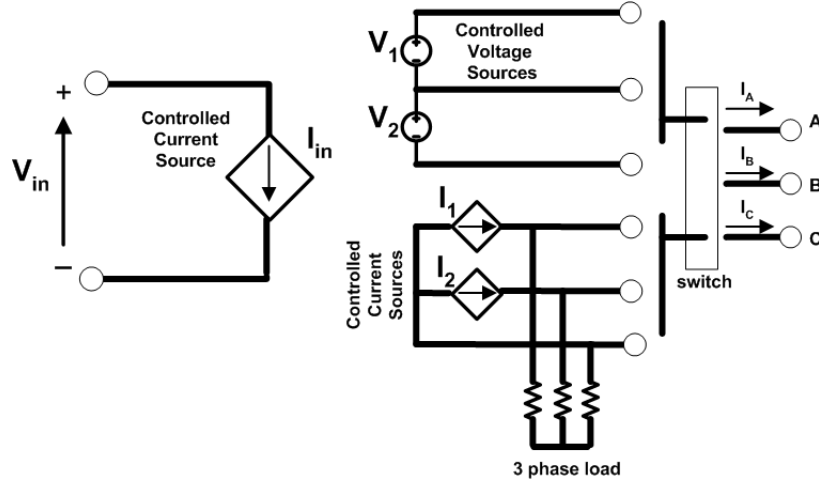


FIGURE 13. Three-phase inverter switching elements average switch model

Three-phase inverter average switch model is shown in Figure 13. Three conditions are required to consider such as power transmission from inverter to motor that is saturated/unsaturated and power transmission from inverter to DC/DC converter. As shown in Figure 13, DC bus side of inverter is represented by a controlled current source while motor side is represented by two controlled current or voltage sources depending on the condition that inverter input DC voltage V_{in} saturates motor or not. Since neutral point electric potential of motor's wye connected stator windings are zero, it is possible to represent inverter's motor side by two controlled sources. Accordingly, following three-phase current and voltage equations are yielded as in Equations (9) and (10).

$$I_A + I_B + I_C = 0 \quad (9)$$

$$V_A + V_B + V_C = 0 \quad (10)$$

Inverter DC bus side controlled current source's input current I_{in} is given by Equation (11). Here, P_{loss} is inverter's switching components' loss power and P_{out} is inverter output power. R_{on} is IGBT on-state resistance.

$$I_{in} = \frac{P_{out} + P_{loss}}{V_{in}} \quad (11)$$

$$P_{out} = V_{AC} * I_A + V_{BC} * I_B \quad (12)$$

$$P_{loss} = (I_A^2 + I_B^2 + I_C^2) * R_{on} \quad (13)$$

In unsaturated motor case, since motor winding currents follow motor reference current signals with almost no error, motor currents are represented by controlled current sources. In other words, two controlled current source currents at motor side represent U and V phase motor reference currents I_1 and I_2 respectively. In saturated motor case, since motor winding currents are not able to follow motor reference current signals successfully, motor currents are favorably represented by V_1 and V_2 generated by two controlled voltage sources. V_1 and V_2 voltages are controlled by a current regulator which generates pulse waves depending on the gap between motor reference current signals and motor winding current signals. In other words, this current regulator tries to keep motor in unsaturated region by turning supply voltage on and off by using pulse waves. This method is also called hysteresis comparator method. $PL1$ and $PL2$ are pulse waves generated by current regulator.

$$V_1 = PL1 * V_{in} \quad (14)$$

$$V_2 = PL2 * V_{in} \quad (15)$$

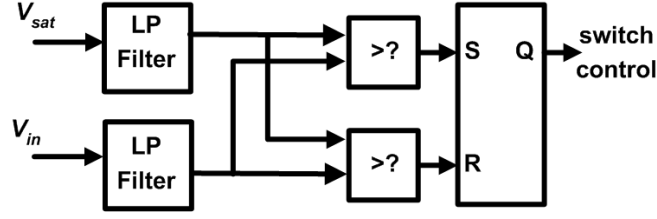


FIGURE 14. Motor saturation detection mechanism

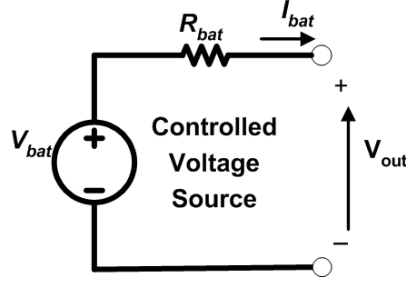


FIGURE 15. Battery model equivalent circuit

Motor saturation detection mechanism which is shown in Figure 14 compares inverter input voltage V_{in} and motor saturation voltage V_{sat} which generate 1 or 0 for the switch in order to select either two controlled current sources or two controlled voltage sources. Consequently motor is fed by one group of controlled sources.

3.3.3. Battery modelling. Battery pack in this model is a 200 V, 6.5 Ah, 21 kW Nickel-Metal-Hydrde (NiMH) ready-to-use generic model [13,27]. As can be seen in Figure 7, it is connected to bidirectional DC/DC converter ends so as to discharge/charge depending on the vehicle running conditions to feed the motor and/or to store regenerative braking power respectively. When modelling the battery, parameters which are obtained from manufacturer's data sheets are referred to and battery is simply modelled by a controlled voltage source and a resistance connected in series is shown in Figure 15. Battery non-linear charge/discharge characteristics approximation is determined using Equation (16). While the battery terminal voltage is calculated using Equation (17) as follows.

$$V_{bat} = V_0 - K \frac{Q}{Q - \int_0^t I_{bat} dt} + A e^{-B \int_0^t I_{bat} dt} \quad (16)$$

$$V_{out} = V_{bat} - I_{bat} R_{bat} \quad (17)$$

In this model, internal resistance R_{bat} is assumed to be constant and parameters shown in Table 2 are the same for both during and charge/discharge of the battery. Moreover, Peukert, temperature and self-discharge effects are neglected. Equation for battery *SOC* is given in Equation (18).

$$SOC = 100 \left(1 - \frac{Q * 1.05}{\int I_{bat} dt} \right) \quad (18)$$

3.3.4. EDLC modelling. In the literature, there can be found several methods for modelling EDLC physical behaviour. Since it is a low voltage device and is offering very high capacitances, traditional modeling methods for capacitor behaviors are not of enough accuracy and adequacy to describe EDLC performance [9]. Therefore, when referring to EDLC modelling methods, classical equivalent method in [28], three branch model in [29]

TABLE 2. Battery parameters

Parameter	Meaning	Unit
V_{bat}	Nominal Voltage	V
V_0	Initial Voltage Constant	V
K	Polarisation Voltage	V
Q	Battery Discharge Capacity	Ah
A	Voltage Coefficient for Exp. Function	V
B	Capacity Coefficient for Exp. Function	(Ah) ⁻¹
$\int I_{bat} dt$	Actual Battery Charge	Ah
I_{bat}	Battery Current	A
R_{bat}	Battery Internal Resistance	Ω

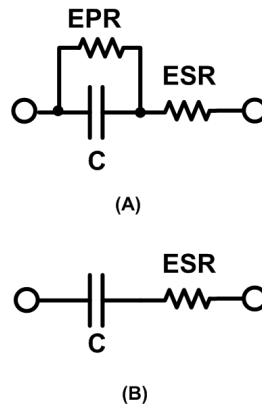


FIGURE 16. (A) Equivalent circuit model of EDLC with EPR (B) equivalent circuit model of EDLC

and porous electrodes as transmission lines method in [30] come into prominence among others. However, in this study, classical equivalent method which is suggested by Spyker and Nelms is used since it is the most simple and famous modelling method. They claim that classical equivalent circuit for EDLC which is composed of capacitance (C), an equivalent parallel resistance (EPR) and an equivalent series resistance (ESR) can accurately model EDLC behavior as shown in Figure 16. In this method, distributed parameters system is used to describe the double-layer capacitor's complex physical nature. According to [31,32], in power electronics applications where capacitor slowly discharges over a few seconds, classical equivalent method can be adopted to predict system behavior although it is a simple model. Here EPR models internal heating in capacitor causing losses. EPR represents the current leakage effect and has effect only in long term performance of EDLC. Since very large time constants and resistances are encountered when measuring attempts of EPR, it is understood that it can be neglected so the model turns out to be like in Figure 16(B). When measuring EPR, EDLC is slowly charged to its rated voltage then waits for a long amount of time t to measure the terminal voltage. Here in Equation (19), V_i and V_f are respectively initial and final voltages and C is the rated capacitance.

$$EPR = -\frac{t}{\ln\left(\frac{V_i}{V_f}\right)C} \quad (19)$$

ESR can also be calculated simply as the ratio of change in the voltage and change in the current during EDLC discharge.

$$ESR = \frac{\Delta V}{\Delta I} \quad (20)$$

Lastly, when determining C in the model, energy change (ΔE) during charge and discharge of EDLC is taken into account.

$$C = \frac{2\Delta E}{V_i^2 - V_f^2} \quad (21)$$

3.3.5. *Hybrid power source model.* A hybrid power source which is composed of an electrochemical battery and EDLC connected in parallel in order to suppress short circuit effect and provide better power flow and a longer life-time for the battery pack is proposed in this work. From this aspect, for the improvement of power source and accordingly the performance of a HEV, EDLC is a highly preferable device which has a high specific power ratio completing the disadvantage of a typical electrochemical battery that has higher energy density when comparing with EDLC. However, EDLCs are not suitable for primary power source use unlike batteries in HEV applications. Figure 17 shows the proposed EDLC system connected in parallel to the battery pack of HEV.

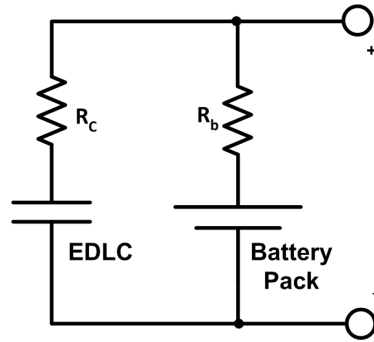


FIGURE 17. Proposed circuit model of EDLC-Battery hybrid power source

Furthermore, developments of vehicle use ultra-capacitors started more than 100 years ago with a goal of achieving at least 5 Wh/kg energy density for high power density discharges and 500,000 deep discharge cycles [33]. Selection of EDLC has been made based on commercially available ones in present that come with quite large capacitances of 1000-5000 F and that are suitable for high power vehicle applications. Table 3 shows the performance of modern and cutting edge technology commercial super capacitors suitable for wide application areas.

For the realization of performance check on EDLC connected HEV, capacitance and equivalent series resistance (ESR) parameters obtained from commercially available Nesscap multi-cell EDLC modules with operating voltages that are within the range of HEV battery pack terminal voltage are utilized. In Table 4, parameters of some Nesscap multi-cell EDLC modules are given. These standardized multi-cell EDLC modules can simply be connected in series to meet the demanded voltage requirements. Their major application areas include automotive applications as well.

$$R_c(ESR) = n * R_{cell} \quad (22)$$

$$V_{DC} = n * V_{cell} \quad (23)$$

$$C_{EDLC} = \frac{C_{cell}}{n} \quad (24)$$

TABLE 3. Commercially available capacitor properties [34]

Manufacturer	Capacitance (F)	Voltage (V)	ESR (m Ω)
P. S. China	50	2.7	–
	300	2.7	–
	600	2.7	1
Panasonic	0.022-70	1-5.5	200-350
Maxwell	63	125	18
	94	75	15
Vinatech	10-600	2.3	20-400
	3-350	2.7	8-90
Nesscap	33	15	27
	51	340	19

TABLE 4. Nesscap EDLC modules for automotive applications

Module	Capacitance (F)	DC Voltage (V)	ESR (m Ω)	Cell nu. (n)
EDLC1	7.2	240	65	5
EDLC2	8.3	208	56	13
EDLC3	13.2	240	50	5
EDLC4	15.4	208	45	13
EDLC5	17.6	240	44	5
EDLC6	20.7	256	38	4
EDLC7	22.2	240	35	5
EDLC8	25.6	208	31	13
EDLC9	31.2	256	30	4
EDLC10	33.2	240	28	5
EDLC11	38.5	208	25	13

3.4. Short circuit modelling. In this study model, short circuit phenomenon is simulated according to the case of the large-gauge cross connection cables which connect the four batteries caused the insulation failure. Therefore, according to the inspection of the battery after the battery breakdown occurs, it is concluded that short circuit is most likely the result of a loose connection of batteries in HEV electrical subsystem. This connection was found to have a nearly 0.16 inch (4.06 mm) gap between the head and the lug that caused arcing [5].

For modelling short circuit fault occurred in the battery pack of HEV, electric arc characterization which is mentioned in [35] has been referred to. Ammerman and his friends postulate that short circuits resulting in arcing can be modelled through this method. One can also find most commonly published and utilized arc equations and developments for dc-arc-resistance models. Physical properties of arcs are hard to comprehend and define. Therefore, the only information related to arc physics is based on the observation and analysis of electrical measurements obtained in empirical works. Since volt-ampere (V-I) characteristics are indispensable to characterize the arc phenomenon, modelling of

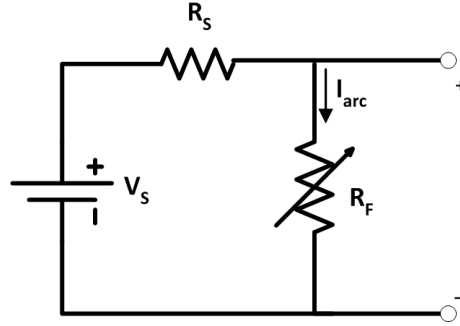


FIGURE 18. Short circuit equivalent model

TABLE 5. Empirical arc formulas for I_{arc}

Electrode Gap (mm)	Arc Voltage (V)	Arc Resistance (Ω)
1	$36.32I_{arc}^{-0.124}$	$36.32I_{arc}^{-1.124}$
5	$71.39I_{arc}^{-0.186}$	$71.39I_{arc}^{-1.186}$
10	$105.25I_{arc}^{-0.239}$	$105.25I_{arc}^{-1.239}$
20	$153.63I_{arc}^{-0.278}$	$153.63I_{arc}^{-1.278}$
50	$262.02I_{arc}^{-0.310}$	$262.02I_{arc}^{-1.310}$
100	$481.20I_{arc}^{-0.350}$	$481.20I_{arc}^{-1.350}$
200	$662.34I_{arc}^{-0.283}$	$662.34I_{arc}^{-1.283}$

mentioned short circuit fault is realized through static V-I characteristics shown in Figure 18. Here, V_S and R_S are the DC source voltage and resistance respectively. R_F and I_{arc} are fault (or arc) resistance and arc current respectively.

Furthermore, Paukert gathered and published arching fault data from several researchers who realized a wide range of arc experiments on DC and single phase arcs then he formulated arc voltage and arc resistance equations for several electrode gap widths [36]. Thus, based on the empirical equivalent short circuit model shown in Figure 18 and formulated arc voltage and arc resistance equations listed in Table 5, corresponding arc resistance and voltage are selected for electrode gap of 5 mm and short circuit simulation model is developed and shown in Figure 19. Also, calculated fault resistances for each current value are given in Table 6. These fault resistance values are utilized when conducting the simulation in order to analyze the HEV performance.

4. Simulation and Results. In simulations, newly designed EDLC-Battery pack hybrid power source on short circuit faults applied HEV simulation model is tested. The HEV configuration with EDLC-Battery pack hybrid power source is shown in Figure 20.

This simulation is developed in Matlab/Simulink environment and runs for 14 sec. During this time, acceleration signal is applied for the first 9 sec, then system switches to deceleration and goes for the next 5 sec. Some performance parameters for the EDLC connected hybrid power-train system under short circuit faults are monitored according to the given simulation conditions during the simulation time. These performance parameters include engine power, generator power, battery power, motor power, capacitor power, EDLC-Battery pack DC bus voltage, battery current, capacitor current, battery pack (SOC) and battery stress factor (SF).

TABLE 6. Calculated fault resistances

Fault Current (A)	Fault Resistance (Ω)
1	71.4
10	46.5
20	40.9
30	37.9
40	35.5
50	34.5
60	33.3
70	32.3
80	31.5
90	30.9
100	30.3

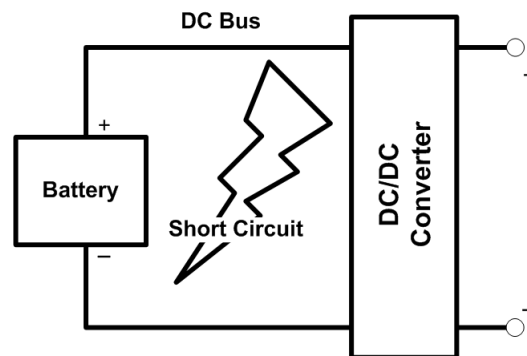


FIGURE 19. Short circuit simulation model

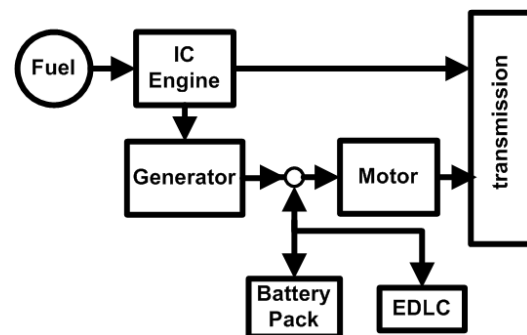


FIGURE 20. Drive-train system with EDLC

They are examined carefully and the change in the performance conditions of the vehicle is interpreted. As shown in Figure 21, when there is no EDLC module connected to the battery pack of HEV, during engine start phase (0 to 0.8th sec), since the vehicle is run only on motor, generator's electricity generation is zero. Between 0.8th sec and 9th sec, vehicle is run on motor and generator both. Therefore, power to the motor is supplied by battery and generator in the same time. However, in the vicinity of 0.8th sec which is the engine start phase, in order to supply required motive force for the start of engine, generator is operated as motor. So at 0.8th sec, generator's drive torque becomes temporarily positive. After the start phase of engine, generator's drive torque switches to negative and generator

starts to generate electricity. After 3.3rd sec, as the required power to drive the motor gets fixed, so does the generator’s output power. During deceleration between 9th and 14th sec, operations of engine and generator are halted. Motor is operated as generator and regenerates electric power from the lost kinetic energy during the deceleration of the vehicle.

Moreover, in case of short circuit, battery current is relatively smaller during the deceleration than during the acceleration. Short circuit also effects the battery state of charge (SOC) as shown in Figure 24. When the short circuit fault is applied, battery discharges less than the normal case. Since vehicle speed during the fault is less than the normal case, discharged power from the battery is less than normal case as well. Because supplied power to the system is less than the normal case, it is clear that short circuit causes vehicle speed to decrease so does the oscillation power flow in the power-train. As a result, in the fault case, speed peak decreases relatively during the acceleration while vehicle tends to consume more fuel during the deceleration.

Table 7 gives energy conditions of electrical subsystem components depending on the calculated fault current and fault resistances in Table 6. From the energy trends of engine, generator, battery and motor, it can be easily seen that a certain amount of energy is lost by short circuiting during acceleration and deceleration of the vehicle [15]. The

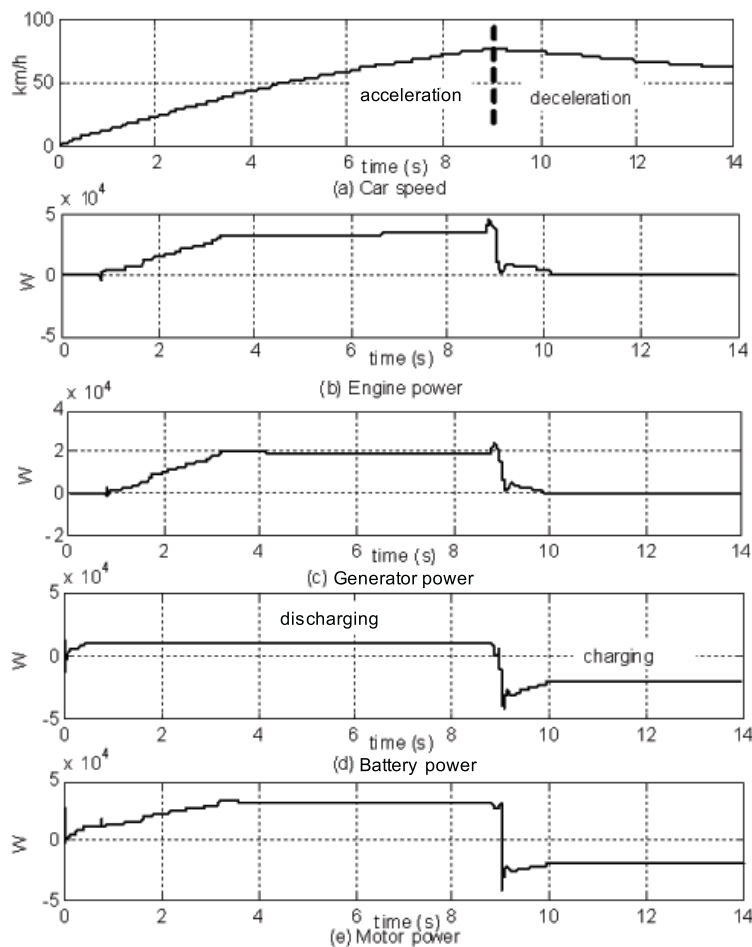


FIGURE 21. Car speed and power during normal operation

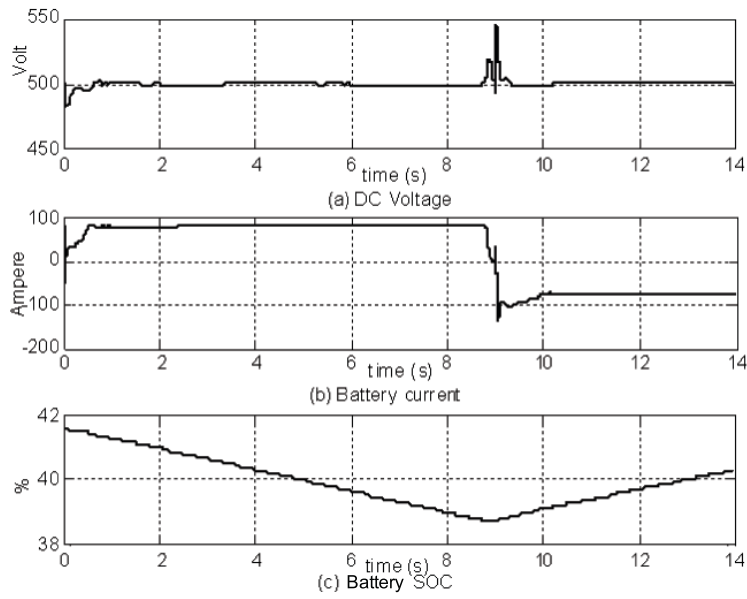


FIGURE 22. DC bus and battery conditions during normal operation

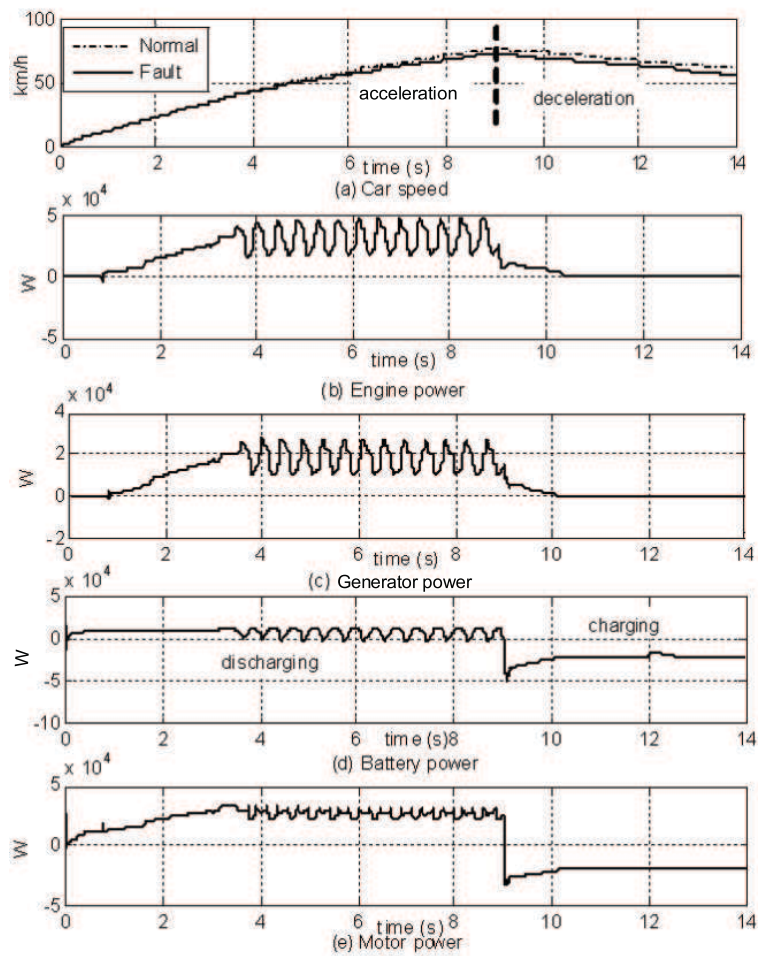


FIGURE 23. Car speed and power during short circuit faulted operation

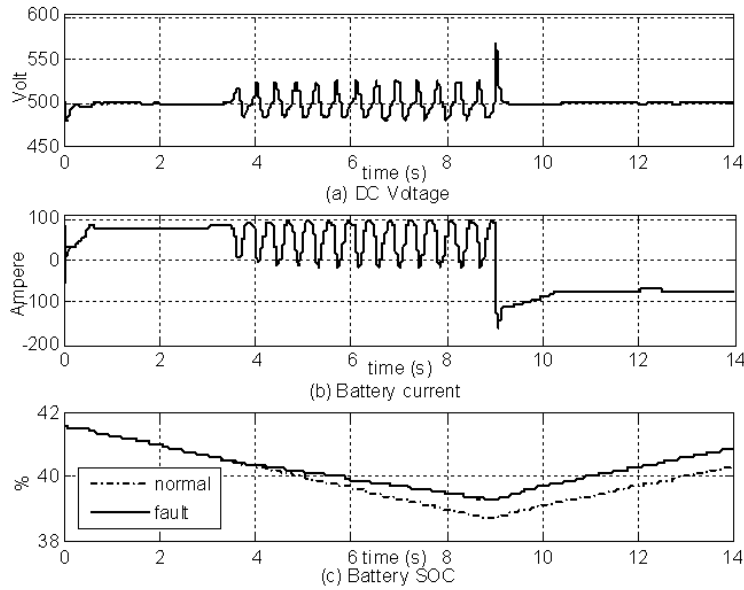


FIGURE 24. DC bus and battery conditions during short circuit faulted operation

TABLE 7. Energy conditions of electrical subsystem components depending on the fault current

Fault Current (A)	Fault Resistance (Ω)	Car Speed Peak (Km/h)	DC Voltage Pike (V)	Acceleration				Deceleration			
				Engine Energy (Wh)	Generator Energy (Wh)	Battery Energy (Wh)	Motor Energy (Wh)	Engine Energy (Wh)	Generator Energy (Wh)	Battery Energy (Wh)	Motor Energy (Wh)
Normal		76.902	545.1	17270	10369	7656	18016	600	216	-7980	-7748
1	71.39	73.046	564.3	16468	9761	6098	15839	763	306	-8147	-7862
10	46.52	72.999	566.7	16443	9749	6103	15823	791	322	-8167	-7881
20	40.89	72.992	566.9	16440	9748	6105	15820	795	325	-8166	-7883
30	37.92	72.987	567	16438	9748	6105	15819	798	326	-8163	-7884
40	35.95	72.985	567.1	16438	9748	6106	15816	798	326	-8163	-7884
50	34.48	72.983	567.1	16438	9748	6107	15815	799	327	-8161	-7884
60	33.34	72.981	567.3	16436	9747	6106	15818	801	328	-8157	-7885
70	32.39	73.002	548.6	16564	9814	5990	15764	619	224	-7907	-7743
80	31.6	73.004	544.3	16563	9812	5986	15765	618	223	-7895	-7740
90	30.91	73.003	543	16559	9810	5985	15763	619	224	-7891	-7741
100	30.31	72.999	542.7	16555	9808	5985	15763	622	226	-7889	-7742

next case is the proposed system that increases stability by utilizing EDLC. Battery-EDLC hybrid power source is analyzed. Obviously, this hybrid power source topology provides a more balanced and higher energy and power density rates. After testing, all developed simulation models of commercial Nesscap EDLC modules are shown in Table 4, EDLC11 is selected due to its impact on the performance parameters which are mentioned earlier since it gives the best results in term of battery SOC and SF as well. EDLC improves the battery power capability since it behaves like a fast charging discharging buffer unit. Therefore, battery-EDLC combination is capable of providing and absorbing current during acceleration and deceleration of vehicle respectively. This feature of EDLC provides power smoothing effect under short circuit fault. This fact can be seen in Figures 25 and 26. Engine, generator and motor power fluctuations go through a smoothing when the vehicle DC bus experiences two short circuit faults in acceleration and deceleration. Buffer effect of EDLC is visualized in battery power and current. Since EDLC releases

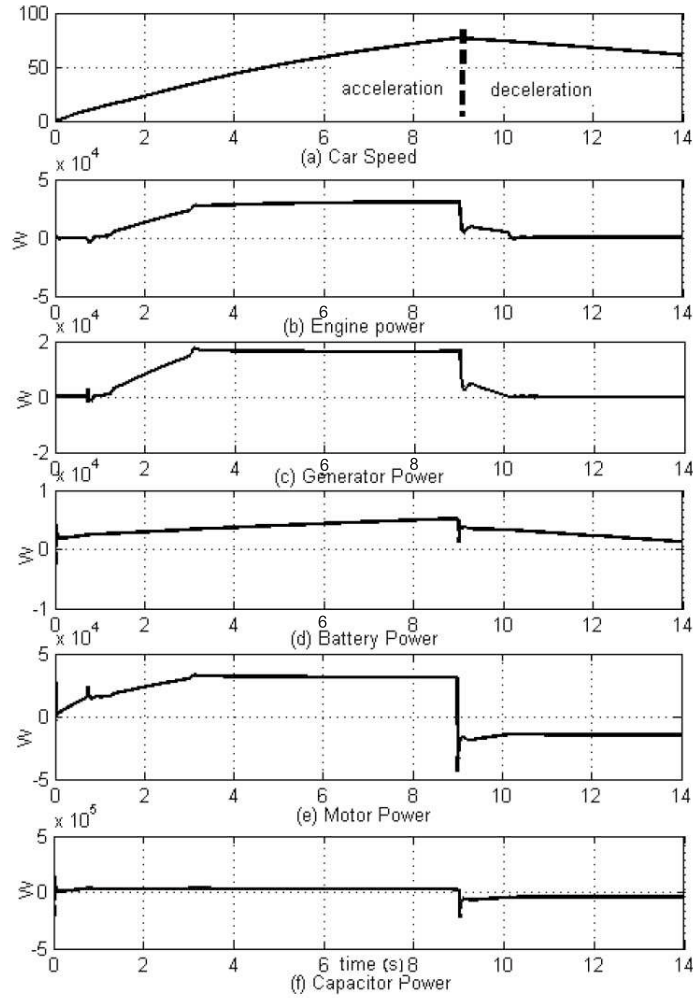


FIGURE 25. Car speed and power during short circuit faulted operation with EDLC

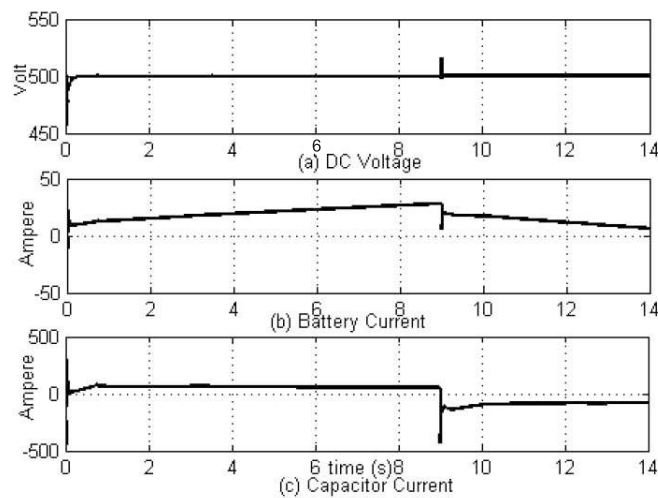


FIGURE 26. DC bus and battery conditions during short circuit faulted operation with EDLC

TABLE 8. EDLC modules vs. battery stress factor

Module	Capacitance (F)	SF (%)
No EDLC	–	100
EDLC1	7.2	45.6
EDLC2	8.3	42.7
EDLC3	13.2	35.3
EDLC4	15.4	32.7
EDLC5	17.6	30.8
EDLC6	20.7	27.8
EDLC7	22.2	27.3
EDLC8	25.6	24.3
EDLC9	31.2	21.7
EDLC10	33.2	20.1
EDLC11	38.5	18.6

and absorbs current very fast, the battery current increases gradually with steps of 1.68 A sec instead of hitting to 80 A in no time as in Figure 22 or 24. Consequently, EDLC fosters battery safety from ruinous failure by short circuit in the system. Accordingly, lifetime of the battery is extended. This fact can also be understood from measured battery Stress Factors which are given in Table 8 after each commercial Nesscap module is connected.

Stress Factor (SF) is defined as a parameter that influences the behavior of the battery performance due to degradation of the chemical process [16]. In this work as an approach to this parameter, impact of high discharge rates to EDLC connected battery pack life time is concerned. Therefore, SF which is a function of battery and load currents is utilized as a measure. This parameter is formulated as in Equation (25) [16]. In Table 8, calculated battery SFs versus each EDLC module are given. As can be seen, when there is no EDLC utilized in the system, the whole burden is on battery pack. Therefore, in this case, SF is 100%. However, while the capacitance value of EDLC modules increases, since the battery current decreases and gradual increase in the current gets slower, battery SF is decreased until 18.6% in case of EDLC11 module.

$$SF = \frac{1}{2} \left(\frac{I_{battery,peak}}{I_{load,peak}} + \frac{\frac{di_{battery}}{dt}}{\frac{di_{load}}{dt}} \right) (\%) \quad (25)$$

Another parameter for monitoring battery lifetime improvement in the system is state of charge (SOC). In Figure 27, condition of SOC for no-EDLC and for each EDLC modules can be seen clearly. From the figure, it can also be understood that the change in SOC during the vehicle's motion gains a smooth trajectory when comparing with no-EDLC case. Obviously, the best SOC performance is obtained when EDLC11 is connected to the system.

5. Conclusions. In this paper, simulation model of a hybrid power source that is comprised of an electrochemical NiMH battery and a super-capacitor (EDLC) connected to each other in parallel is developed. This proposed hybrid power source is tested on a HEV simulation model with short circuit faults encountered in its DC bus of electric subsystem during acceleration and deceleration of the vehicle. We also developed a simulation model for short circuit by using electric arc characterization method. During the simulation based performance tests, a good clearance of short circuit fault effect and consequently a considerable performance enhancement at HEV operation are obtained. As

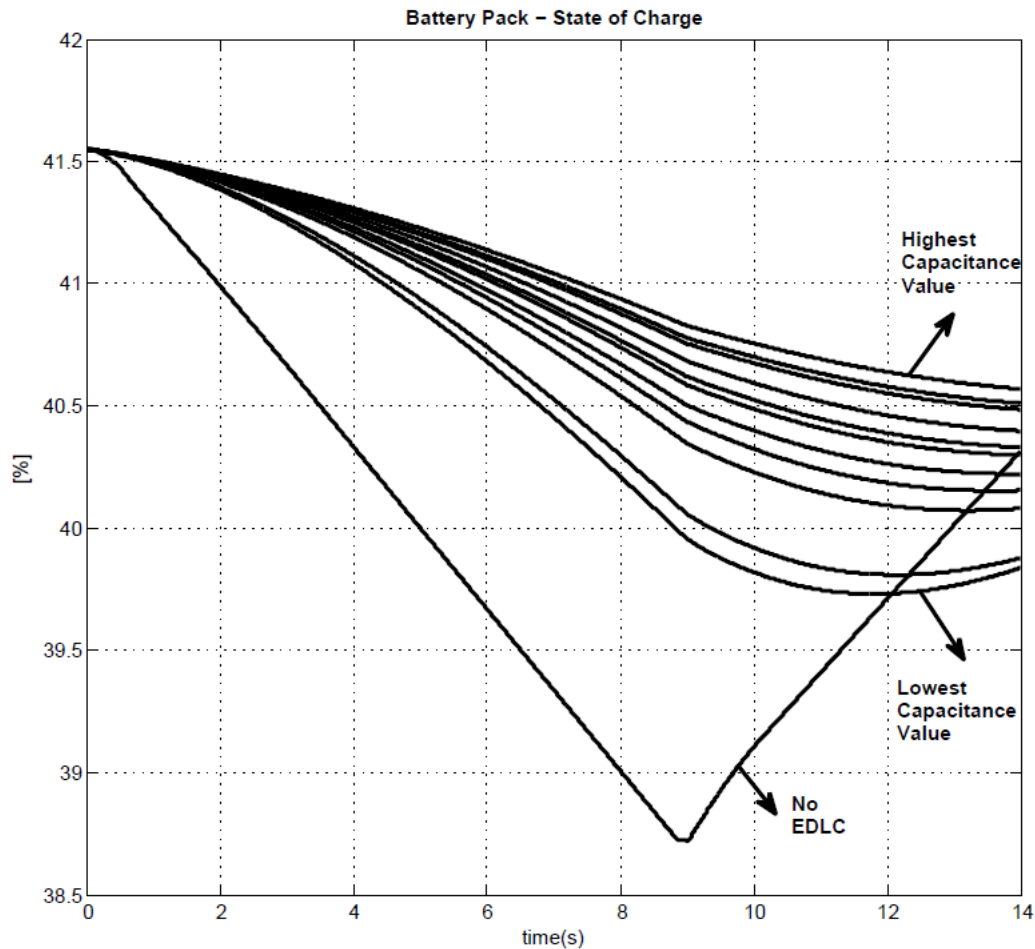


FIGURE 27. Battery state of charge

performance parameters, we considered power/power flow quality in electric subsystem elements such as generator, motor and battery as well as IC engine. Besides, improvement in battery lifetime and performance is also visualized by battery state-of-charge (SOC) and stress factor (SF).

Acknowledgment. The authors gratefully acknowledge to the Directorate General for Higher Education (DGHE or DIKTI), Ministry of National Education of Republic Indonesia and JICA Joint Research PREDICT Program (B-2-4) for supporting this research.

REFERENCES

- [1] *International Energy Agency: CO₂ Emissions from Fuel Combustion*, www.iea.org.
- [2] K. Chau and Y. Wong, Overview of power management in hybrid electric vehicles, *Energy Conversion and Management*, vol.43, no.15, pp.1953-1968, 2002.
- [3] M. Ehsani, Y. Gao and J. M. Miller, Hybrid electric vehicles: Architecture and motor drives, *Proc. of the IEEE*, vol.95, no.4, pp.719-728, 2007.
- [4] Toyota Prius gasoline electric hybrid, *Emergency Response Guide*, 2000.
- [5] G. P. Beauregard, *Report of Investigation: Hybrids Plus Plug-in Hybrid Electric Vehicle*, 2008.
- [6] M. Ishiko, Recent R-D activities of power devices for hybrid electric vehicles, *R-D Review of Toyota CRDL*, vol.39, p.1, 2004.
- [7] K. H. Hussein, G. Majumdar, S. Yoshida and H. Maekawa, IPMs solving major reliability issues in automotive applications, *Proc. of the 16th ISPSD*, pp.89-92, 2004.

- [8] F. V. Conte, P. Gollob and H. Lacher, Safety in the battery design: The short circuit, *World Electric Vehicle Journal*, vol.3, pp.1-8, 2009.
- [9] P. Sharma and T. S. Bhatti, A review on electrochemical double-layer capacitors, *Energy Conversion and Management*, vol.51, no.12, pp.2901-2912, 2010.
- [10] A. F. Burke, Batteries and ultracapacitors for electric, hybrid, and fuel cell vehicles, *Proc. of the IEEE*, vol.95, no.4, pp.806-820, 2007.
- [11] N. Urasaki and M. Iwasaki, Hybrid power source with electric double layer capacitor and battery in electric vehicle, *International Conference on Electrical Machines and Systems*, pp.758-761, 2010.
- [12] E. Tara, S. Filizadeh, J. Jatskevich, E. Dirks, A. Davoudi, M. Saedifard, K. Strunz et al., Dynamic average-value modelling of hybrid-electric vehicular power systems, *IEEE Transactions on Power Delivery*, vol.27, no.1, pp.430-438, 2012.
- [13] O. Tremblay, L. Dessaint and D. Abdel-Allah, A generic battery model for the dynamic simulation of hybrid electric vehicles, *Electrical Engineering*, pp.284-289, 2007.
- [14] M. Ehsani, *Modern Electric, Hybrid Electric, and Fuel Cell Vehicles: Fundamentals, Theory, and Design*, CRC, Boca Raton, FL, USA, 2005.
- [15] S. Ibrahim, A. D. Anton and H. Takashi, Simulation-based analysis of short circuit fault in parallel-series type hybrid electric vehicle, *The International Conference on Advanced Power System Automation and Protection*, 2011.
- [16] N. Omar, J. Van Mierlo, B. Verbrugge and P. Van den Bossche, Power and life enhancement of battery-electrical double layer capacitor for hybrid electric and charge-depleting plug-in vehicle applications, *Electrochimica Acta*, vol.55, no.25, pp.7524-7531, 2010.
- [17] A. C. Baisden and A. Emadi, ADVISOR-based model of a battery and an ultra-capacitor energy source for hybrid electric vehicles, *IEEE Transactions on Vehicular Technology*, vol.53, no.1, pp.199-205, 2004.
- [18] J. Cao and A. Emadi, A new battery/ultracapacitor hybrid energy storage system for electric, hybrid, and plug-in hybrid electric vehicles, *IEEE Transactions on Power Electronics*, vol.27, no.1, pp.122-132, 2012.
- [19] M. Amrhein and P. T. Krein, Dynamic simulation for analysis of hybrid electric vehicle system and subsystem interactions, including power electronics, *IEEE Transactions on Vehicular Technology*, vol.54, no.3, pp.825-836, 2005.
- [20] M. Abul Masrur, Z. Chen and Y. Murphey, Intelligent diagnosis of open and short circuit faults in electric drive inverters for real-time applications, *Power Electronics, IET*, vol.3, no.2, pp.279-291, 2010.
- [21] L. Guzzella and C. H. Onder, *Introduction to Modelling and Control of Internal Combustion Engine Systems*, Springer, New York, USA, 2010.
- [22] A. Emadi, *Handbook of Automotive Power Electronics and Motor Drives*, Taylor-Francis, New York, USA, 2005.
- [23] R. Krishnan, *Electric Motor Drives: Modelling, Analysis, and Control*, Upper Saddle River, Prentice-Hall, NJ, USA, 2001.
- [24] A. Davoudi, J. Jatskevich, P. L. Chapman and A. Khaligh, Averaged-switch modelling of fourth-order PWM DC-DC converters considering conduction losses in discontinuous mode, *IEEE Trans. Power Electron.*, vol.22, no.6, pp.2410-2415, 2007.
- [25] E. Van Dijk, J. N. Spruijt, D. M. OSullivan and J. B. Klaassens, PWM-switch modeling of DC-DC converters, *IEEE Trans. Power Electron.*, vol.10, no.6, pp.659-665, 1995.
- [26] S. Chiniforoosh, J. Jatskevich, A. Yazdani, V. Sood, V. Dinavahi, J. A. Martinez and A. Ramirez, Definitions and applications of dynamic average models for analysis of power systems, *IEEE Trans. on Power Del.*, vol.25, no.4, pp.2655-2669, 2010.
- [27] O. Tremblay and L. Dessaint, Experimental validation of a battery dynamic model for EV applications, *World*, vol.3, pp.1-10, 2009.
- [28] R. L. Spyker and R. M. Nelms, Classical equivalent circuit parameters for a double-layer capacitor, *IEEE Transactions on Aerospace and Electronic Systems*, vol.36, no.3, pp.829-836, 2000.
- [29] L. Zubietta and R. Bonert, Characterization of double-layer capacitors for power electronics applications, *IEEE Trans. on Ind. Appl.*, 2000.
- [30] R. De Levie, On porous electrodes in electrolyte solutions, *Electrochem Acta*, 1963.
- [31] R. L. Spyker, *Application of Double-Layer Capacitors in Power Electronic Systems*, Ph.D. Thesis, Auburn University, 1997.

- [32] R. L. Spyker and R. M. Nelms, Double layer capacitor/dc-dc converter system applied to constant power loads, *Proc. of the 31st Intersociety Energy Conversion Engineering Conference*, pp.255-259, 1996.
- [33] A. F. Burke, Electrochemical capacitors for electric vehicles: A technology update and recent test results from INEL, *The 36th Power Sources Conf.*, Cherry Hill, NJ, USA, 1994.
- [34] P. Jampani and A. Manivannan, Advancing the super-capacitor materials and technology frontier for improving power quality, *Electrochemical Society*, 2010.
- [35] R. F. Ammerman, T. Gammon, P. K. Sen and J. P. Nelson, Dc arc models and incident energy calculations, *Record of Conference Papers – Industry Applications Society the 56th Annual Petroleum and Chemical Industry Conference*, vol.46, no.5, pp.1-13, 2009.
- [36] J. Paukert, The arc voltage and arc resistance of LV fault arcs, *Proc. of the 7th Int. Symp. Switching Arc Phenom.*, 1993.